Signal Analysis Using Fourier-like Wavelets

Luciana R. Soares, *Student Member, IEEE*, H. M. de Oliveira, *Member, IEEE*, and Renato J. S. Cintra

***Abstract*—In continuous-time wavelet analysis, most wavelet present some kind of symmetry. Based on the Fourier and Hartley transform kernels, a new wavelet multiresolution analysis has been proposed. This approach is based on a pair of orthogonal wavelet functions and can be named as the Fourier-like and Hartley-like wavelet analysis. In this paper we carry a preliminary investigation about potentials applications for the Fourier-like wavelet analysis on signals derived from power systems to illustrate the behavior of such wavelets.**

***Index Terms*—analytic wavelets, Fourier transform kernel, Fourier-like wavelets, Hilbert transform, signal analysis, wavelet design, wavelet transform.**

I. Introduction

The idea of comparing Fourier analysis with wavelet decompositions was the starting point for introducing an analysis based on a couple of orthogonal wavelet functions, one with even symmetry and other with odd symmetry. This approach has been named as the Fourier-like and Hartley-like wavelet analysis [1].

In order to allow further investigation on the Fourier-like wavelet analysis, a brief review of the Fourier-like and Hartley-like wavelet analysis [1] is presented. As result it can be shown that the Fourier-like wavelet analysis is similar to the analytical wavelet transform, when using analytical wavelets.

This paper carries a preliminary investigation about applications of the Fourier-like wavelet analysis on signals derived from power systems.

II. The Fourier-like and Hartley-like Wavelet Analysis

In the standard Fourier analysis, a signal $x(t)$ is simultaneously analyzed by even and odd functions, being represented by:

$$x(t) = d.c.\ \text{term} + \textit{cosine}\ \text{terms} + \textit{sine}\ \text{terms}. \tag{1}$$

In the standard wavelet-based multiresolution analysis (WMRA) [2], $x(t)$ may be represented by:

$$x(t) = \varphi\,\text{term} + \psi\,\text{terms}, \tag{2}$$

where "φ term" accounts for the analysis of $x(t)$ with a scaling function $\varphi(t)$, and "ψ terms" represent those ones derived from scaled versions of a mother wavelet function $\psi(t)$.

Comparing the WMRA and the Fourier analysis equations, the scaling coefficients, "φ term", play a role that corresponds to the *d.c.* term of the Fourier series; the wavelet coefficients, "ψ terms", can be viewed as the harmonic components of the Fourier series, since the harmonics are scaled versions of the infinite Fourier kernel.

In a continuous-time wavelet analysis, most available wavelet functions present some kind of symmetry [3]. Hence, it seems natural to associate to each wavelet with even symmetry another one of odd symmetry, and vice-versa. The Hilbert transform is invoked to derive the *in quadrature* version of a symmetric (or an anti-symmetric) wavelet [4], [1]. Hence, $x(t)$ may be represented on a new continuous-time WMRA by:

$$x(t) = \varphi\,\text{term} + \psi\,\text{terms} + \textit{orthogonal of}\ \psi\,\text{terms}. \tag{3}$$

Accordingly, new wavelet functions that look like the Fourier and Hartley transform kernels are invoked. Thus, by analogy to Fourier and Hartley transforms, the "cosine and sine" kernel is replaced by "ψ and Hilbert transform of ψ" in this new concept of wavelet analysis.

A. The Hilbert Transform of Wavelets

A function $\psi(t)$ is a mother-wavelet, *if and only if*, (i) $\psi(t)$ is in the space of finite energy functions $L^2(R)$, and (ii) $\psi(t)$ satisfies the admissibility condition [2].

In [1], some properties have been explored in view of applying the Hilbert transform to wavelets. In particular, it is established that the Hilbert transform of a real wavelet, $Hb\{\psi(t)\}$, is also a real wavelet with same energy, admissibility coefficient and at least same number of null moments than its generating wavelet, $\psi(t)$.

Fig. 1 shows some continuous-time real wavelets and their corresponding Hilbert transforms.

This work was partially supported by Brazilian Ministry of Education (CAPES) and by the Brazilian National Council for Scientific and Technological Development (CNPq) under research grant #306180.

L. R. Soares and H. M. de Oliveira are with the Signal Processing Group, Department of Electronics and Systems, Federal University of Pernambuco – UFPE, C.P. 7800, 50711-970, Recife, PE, Brazil (e-mail: lusoares@ufpe.br, hmo@ufpe.br). R. J. de Sobral Cintra is with the Department of Statistics of the same university (e-mail: rjdsc@de.ufpe.br).

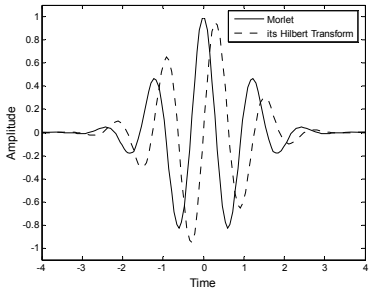

(a)

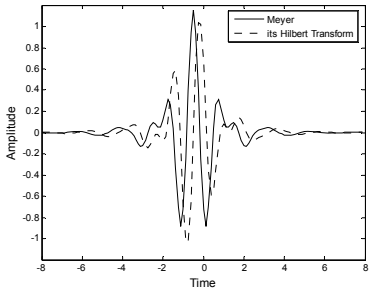

(b)

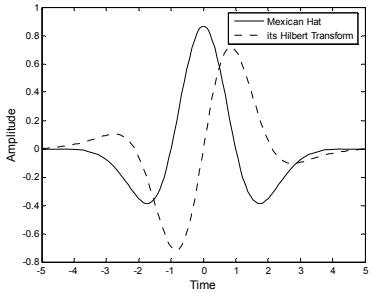

(c)

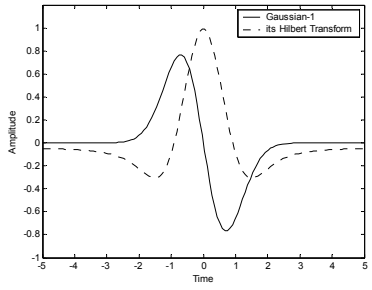

(d)

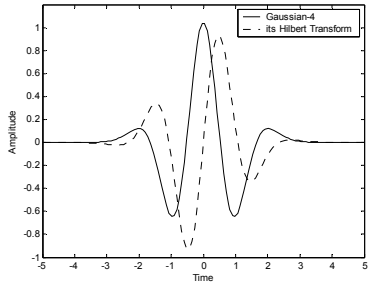

(e)

Fig. 1. Continuous-time wavelets and their Hilbert transforms: (a) Morlet; (b) Meyer; (c) Mexican Hat; (d) Gaussian-1; (e) Gaussian-4.

B. The Fourier Kernel on the Wavelet Analysis

The Fourier transform kernel, or Fourier kernel, is defined by $e^{j\cdot t} = \cos(t) + j\cdot\sin(t)$. Evoking that $Hb\{\cos(t)\} = -sin(t)$, then the Fourier kernel can also be written as $e^{j\cdot t} = \cos(t) - j\cdot Hb\{\cos(t)\}$.

This quite naive observation has motivated the definition of Fourier-like wavelets, $Ft\{\psi(t)\}$, based on a real wavelet and its Hilbert transform [1]:

$$Ft\{\psi(t)\} = \frac{1}{\sqrt{2}}\cdot\left(\psi(t) - j\cdot Hb\{\psi(t)\}\right). \tag{4}$$

Thus, a Fourier-like wavelet, $Ft\{\psi(t)\}$, is a complex wavelet with same energy, admissibility coefficient and also N vanishing moments as its generating wavelet, $\psi(t)$.

In the frequency domain, Fourier-like wavelets are null for $\omega > 0$. For $\omega < 0$, they have the magnitude response of the generating wavelet multiplied by a scalar factor. This is a special behavior of analytical signals [5].

III. Example Cases Using Fourier- like Wavelets

In this section we carry a preliminary investigation about potentials applications of the Fourier-like wavelet analysis on signals derived from power systems so as to illustrate the behavior of the proposed wavelets.

Consider the wavelet transform, $C_{a,b}$ coefficients, given by:

$$C_{a,b} = \frac{1}{\sqrt{a}}\cdot\int_{-\infty}^{+\infty} f(t)\cdot\psi^*\left(\frac{t-b}{a}\right)dt, \tag{6}$$

where $\psi^*(.)$ is the complex conjugate of the mother wavelet $\psi(.)$, a $(a>0)$ and b are, respectively, real scale and translation scalars, and $f(t)$ is the signal under analysis.

A. Multiple Events Analysis

Fig. 2 shows the voltage signals derived from a real voltage disturbance in a three phase power system.

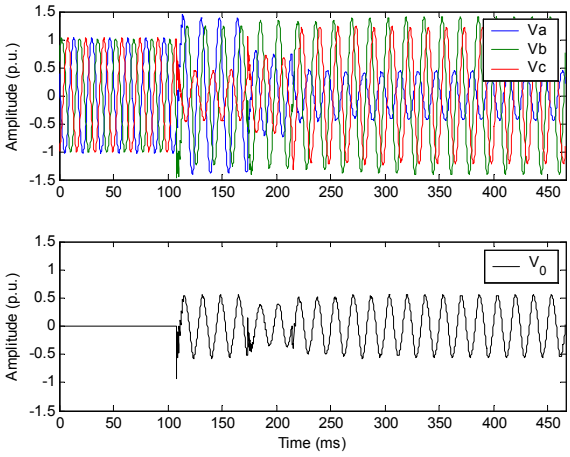

Fig. 2. Voltage signals (**a**, **b**, **c** phases and **0** mode) derived from a real voltage disturbance in a three-phase power system.

This signal corresponds to a multiple event derived from consecutive and different fault conditions: (1) **c** phase to earth fault; (2) two-phases to earth fault; (3) **a** phase to earth fault. The ground involvement in all events can be verified by the **0** mode voltage created after the first fault condition and its maintenance in the successive events.

This event can also be named an evolving fault and the timestamps when different fault conditions occur can be estimated by appropriated wavelet and scale parameter choices.

Fig. 3 shows the time-scale charts of a 64-level wavelet transform of Fig. 2 signals using the Fourier-like Gaussian-4 wavelet and integer scale parameters ranging from 1 to 64. In these graphs, the x-axis represents position along the signal (time), the y-axis represents scale, and the color at each x-y point represents the magnitude of the wavelet coefficient. The colors are scaled between zero (black) and the maximum absolute value of the coefficients.

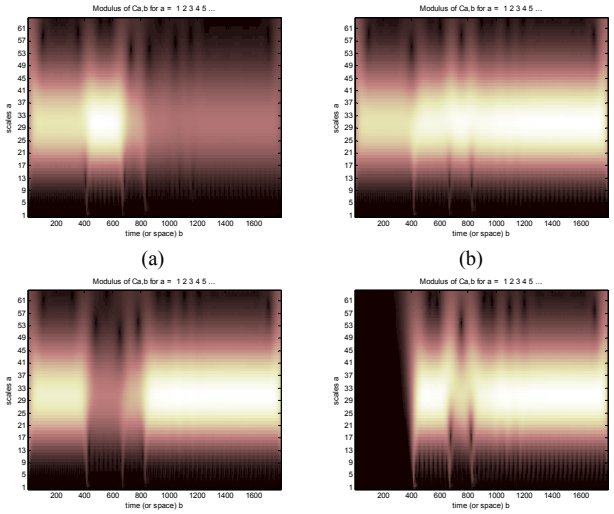

Fig. 3. Magnitude of the wavelet coefficients of Fig. 2 signals using the Fourier-like Gaussian-4 wavelet and integer scale parameters ranging from 1 to 64: (a) phase **a**; (b) phase **b**; (c) phase **c**; (d) mode **0**.

At lower scales, the voltage disturbance occurrences can be identified by abrupt magnitude transitions on the time-scale plane. As the higher wavelet coefficients are concentrated at the mid-range scales, the envelope of approximated versions of Fig. 2 signals can be attained within it, as we are using a complex wavelet.

Fig. 4 shows the magnitude of the resulting complex signals derived from the 5th and 21st wavelet transform levels. Using a threshold on the signals depicted in Fig. 4-(a), the disturbance intervals can be easily obtained. The beginning of each interval is indicated in Fig. 5 by the timestamp of the first of the four signals to reach the threshold. As a consequence, we can perform the system analysis for each one of the three intervals. In Fig. 4-(b), voltage sags reaching about to 45%, 55% and 45% of the pre-fault condition can be identified for each one interval.

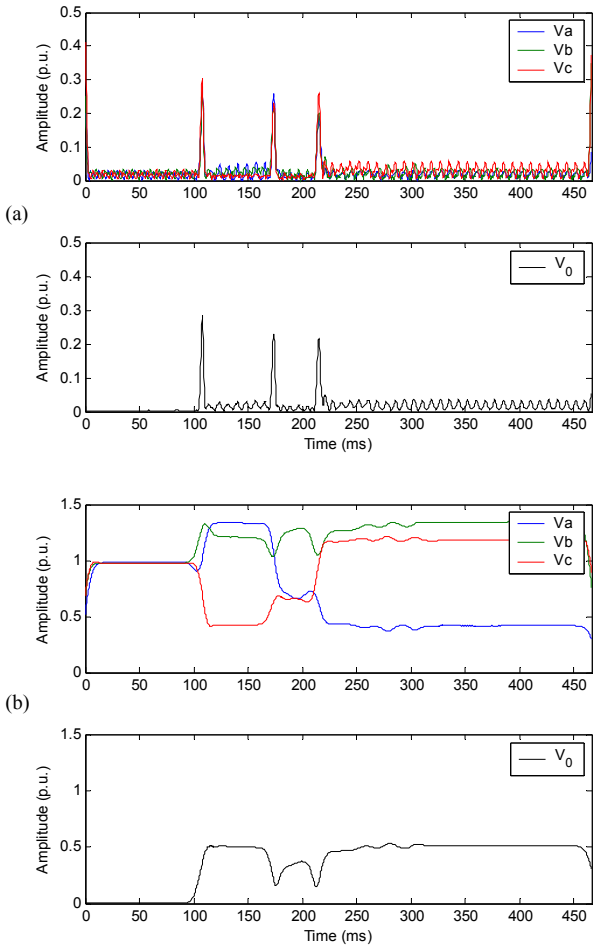

Fig. 4. Absolute values of the wavelet coefficients of Fig. 2 signals using the Fourier-like Gaussian-4 wavelet: (a) $a = 5$; (b) $a = 21$.

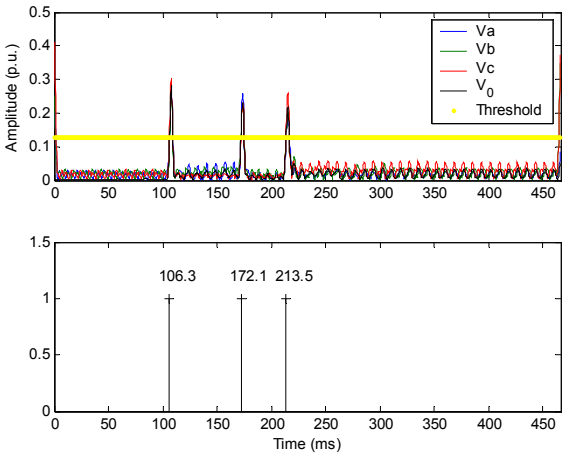

Fig. 5. Intervals identification between consecutive events.

B. *Fault Analysis on Transmission Lines*

Fig. 6 shows the voltage and current signals derived from a simulated three-phase fault on a transmission line at 51.4km from the monitoring terminal [6].

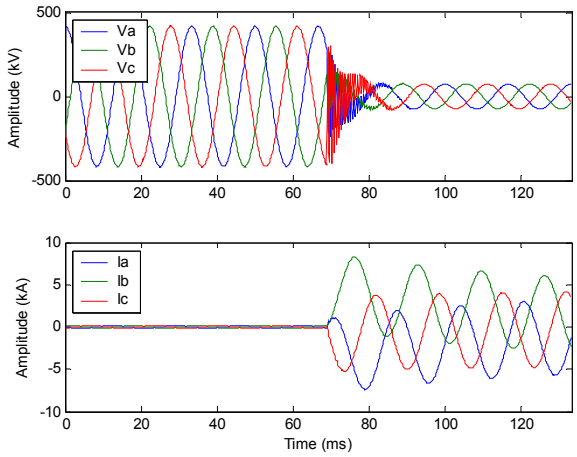

Fig. 6. Voltage and current signals derived from a simulated three-phase fault on a transmission line at 51.4km from the monitoring terminal.

The proper selection of a mother wavelet and a scale parameter may identify approximated versions of the fundamental (60 Hz) voltage and current signals avoiding the transient (high-frequency) signals. As the wavelet transform naturally filters the d.c. decaying of the current signals, these parameters (transient and d.c. values) do not influence in the fault location estimation.

The fault location on a transmission line can be estimated by the apparent impedance approach [7]. When a fault involves more than one phase, as in this example case, the fault impedance can be obtained by [7]:

$$Z_F = \frac{V_X - V_Y}{I_X - I_Y}, \tag{7}$$

where Z_F is the apparent impedance measured at the monitoring terminal, V and I are the fundamental components of the voltage and current signals, and X and Y are the involved phases on the fault. For three phase faults, it can be used any phases combinations.

The fault distance from the monitoring terminal, D_F, can be estimated by:

$$D_F = \frac{Z_F}{Z_1}, \tag{8}$$

where Z_1 is the transmission line positive sequence impedance (Ω/km).

Instead of using the fundamental components of the voltage and current signals (frequently attained by Fourier transforms), we propose the replacement of V and I by the complex voltage and current signals, considering that the fundamental components of such signals can be selected by a proper choice of the wavelet transform level.

Fig. 7 shows the magnitude and phase time-scale charts of a 64-level wavelet transform of phase **a** signals using the Fourier-like Mexican Hat wavelet and integer scale parameters ranging from 1 to 64. The **b** and **c** phase signals present similar time-scale charts.

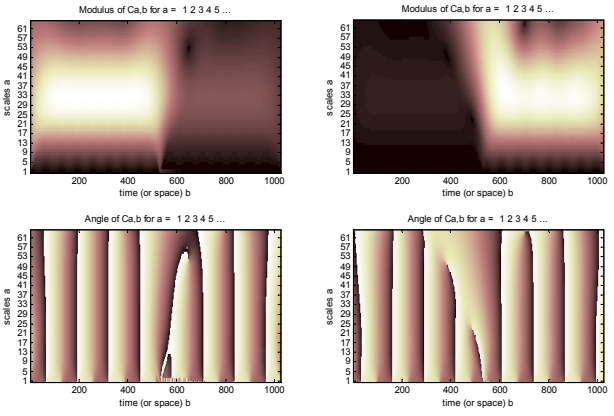

(a) (b)

Fig. 7. A 64-level wavelet analysis of phase **a** signals of Fig. 6 using the Fourier-like Mexican Hat wavelet and integer scale parameters ranging from 1 to 64: (a) voltage; (b) current.

Fig. 8 shows the real, imaginary and absolute values of the phase **a** signals at the 32nd scale. It can be seen that the transient signal on this voltage signal and the exponential decaying on the current signal are not present in these approximated versions of the original signals.

In Fig. 9, the magnitude and angle phase values of all three phase signals derived from the 32nd-level wavelet transform are shown. It can be seen the voltage sag reaching about to 20% of the pre-fault value and the phase-shift on the current signals motivated by the fault occurrence. Later feature can be used in a phase selection algorithm [8] for identifying the involved phases on a fault.

As well in the first example case, the disturbance detection can also be attained by lower scale values.

Finally, Fig. 10-(a) illustrates the continuous-time fault distance estimations using the complex 32nd-level wavelet transform signals and (7)-(8) equations. Mean values can also be attained. Fig. 10-(b) shows the moving average of the fault distances using a 128 point-window (1-cycle window).

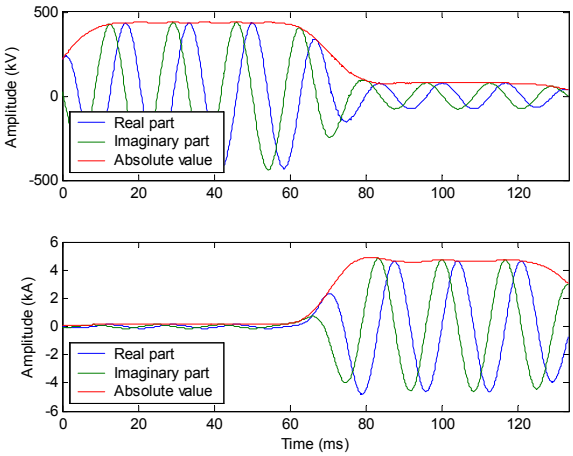

Fig. 8. Real, imaginary and absolute values of the 32nd-level wavelet transform of phase **a** signals using the Fourier-like Mexican Hat wavelet.

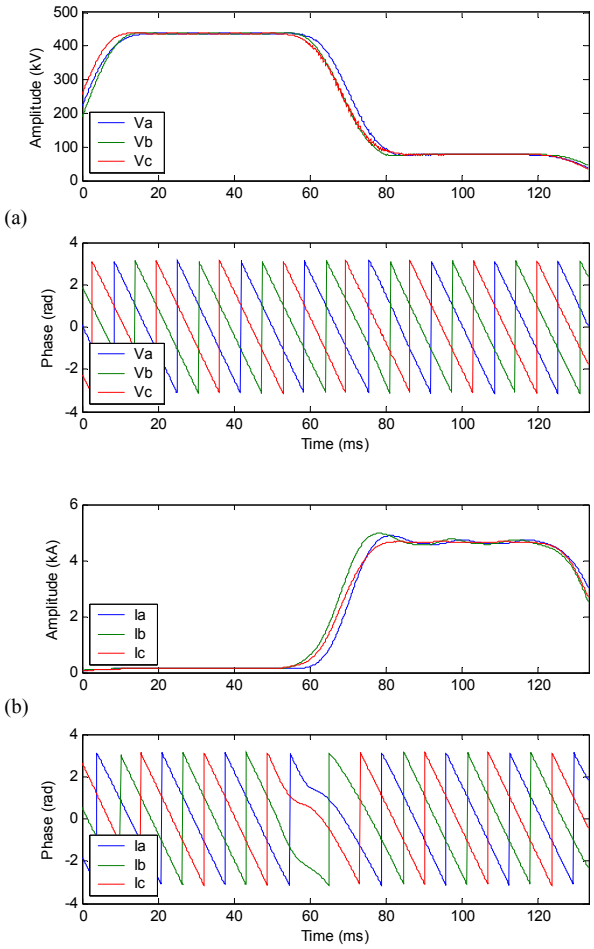

Fig. 9. Absolute and angle phase values of the 32nd-level wavelet transform of Fig. 6 signals using the Fourier-like Mexican Hat wavelet: (a) voltage signals; (b) current signals.

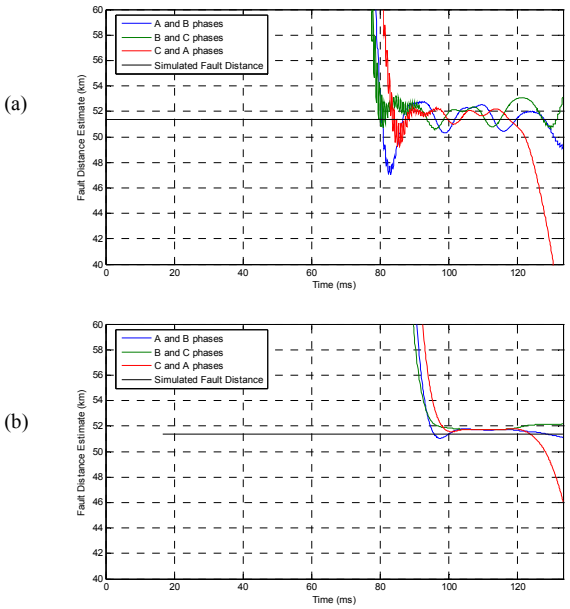

Fig. 10. Fault distance estimation from the monitoring terminal using the Fourier-like Mexican Hat mother wavelet and its 32nd scaling level (a) and using averaged values at each 1-cycle (b).

C. Power Measurements

Fig. 11 shows the voltage and current signals derived from a real single phase to earth fault in a power system. The active and reactive powers at the fundamental frequency can be attained by wavelet transforms, being estimated by appropriated wavelet and scale parameter choices allowing the study of power flows on a transmission line during electrical disturbances.

The single phase active and reactive powers can be attained throughout the complex voltage and current signals by the following expressions [9]:

$$P_i = \left|C_{a,b}(V_i)\right| \cdot \left|C_{a,b}(I_i)\right| \cdot \cos(\theta), \tag{9}$$

$$Q_i = \left|C_{a,b}(V_i)\right| \cdot \left|C_{a,b}(I_i)\right| \cdot \sin(\theta), \tag{10}$$

where $\theta = \angle(C_{a,b}(V_i)) - \angle(C_{a,b}(V_i))$, $i = \mathbf{a}, \mathbf{b}, \mathbf{c}$ phases.

Fig. 12 shows, as an example, the magnitude and phase time-scale charts of a 64-level wavelet transform of phase **a** signals using the Fourier-like Morlet wavelet and integer scale parameters ranging from 1 to 64.

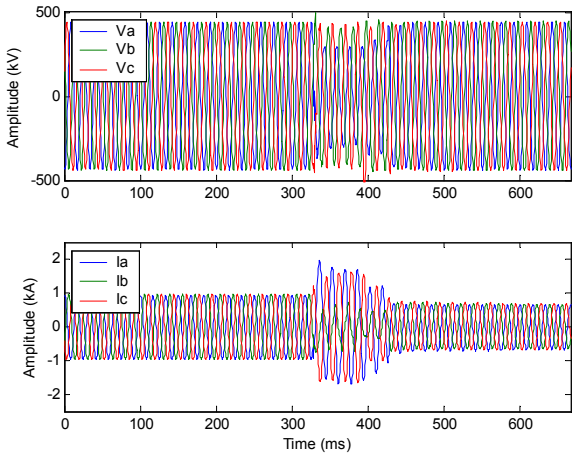

Fig. 11. Voltage and current signals (**a**, **b**, **c** phases) derived from a real voltage disturbance in a three-phase power system.

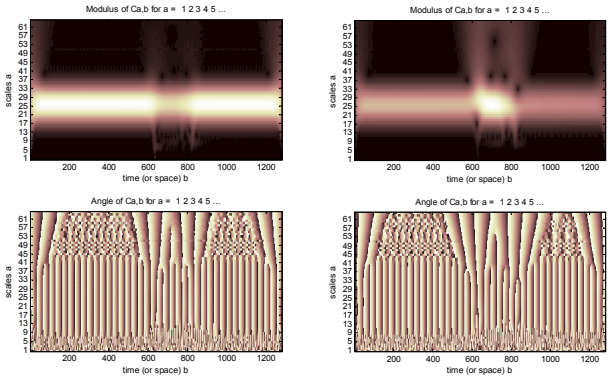

Fig. 12. A 64-level wavelet analysis of phase **a** signals of Fig. 12 using the Fourier-like Morlet wavelet and integer scale parameters ranging from 1 to 64: (a) voltage; (b) current.

At the mid-range scales, we can attain the envelope of approximated versions of Fig. 11 signals. In Fig. 13, the magnitude values of the resulting complex signals derived from the 26th-level wavelet transform of all three phase signals are shown. This figure also includes an estimate of the active and reactive powers using (9)-(10) equations. A reactive power flow reversal can be observed during the fault condition for that monitoring terminal.

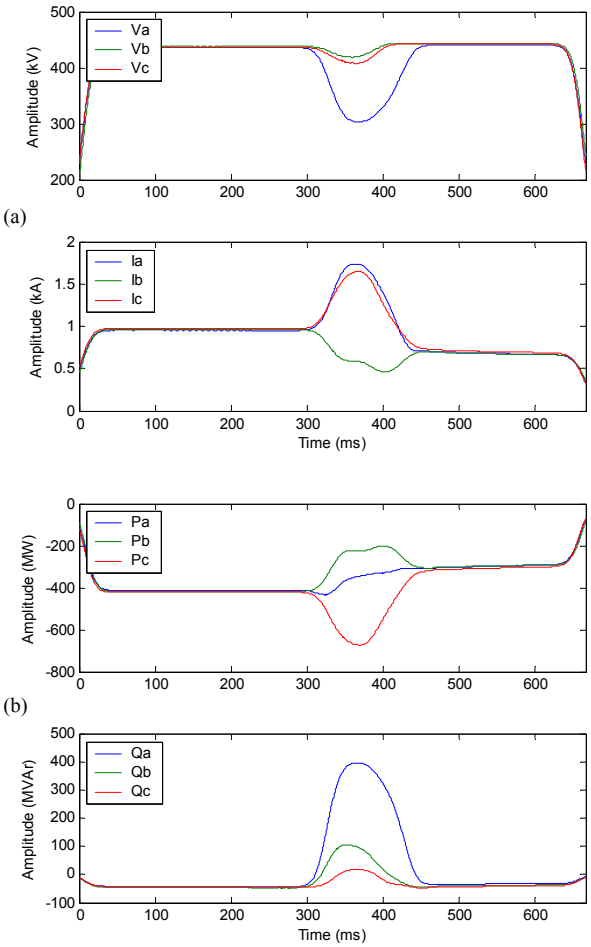

Fig. 13. Absolute values of the 26th-level wavelet transform of Fig. 12 signals using the Fourier-like Morlet wavelet: (a) voltages and currents; (b) active and reactive powers.

IV. Conclusions

Impelled by an analogy between Fourier and wavelet transform kernels, the Fourier-like wavelet analysis was proposed. Fourier-like wavelets have been derived from the Fourier transform kernel, which have been written on the basis of Hilbert transform. Recently, complex wavelets have been proposed for power system analysis. Fourier-like wavelets can be an alternative to those functions, increasing thereby the number of complex wavelets at disposal to researches.

The example cases illustrate that the use of Fourier-like wavelets has applications for power quality analysis in power system. Throughout a complex wavelet analysis, we can derive important characteristics to each one of all three phases' signals: impedance, power factor, phase shifting, and active and reactive powers, to name a few.

A comprehensive study about the frequency response of the continuous-time wavelets and the signals under analysis must be carried out to select the appropriated mother wavelet and wavelet transform level for support the desirable analysis.

V. References

[1] L. R. Soares, H. M. de Oliveira, and R. J. S. Cintra, "The Fourier-like and Hartley-like Wavelet Analysis Based on Hilbert Transforms," *in Annals of the XXII Simpósio Brasileiro de Telecomunicações (SBT'05)*, Campinas, Brazil, Sept. 4-8, 2005.

[2] C. K. Chui, *An Introduction to Wavelets*, San Diego, CA: Academic Press, 1992.

[3] M. Misiti, Y. Misiti, G. Oppenheim, and J.-M. Poggi, *Wavelet Toolbox User's Guide*, New York: The MathWorks, Inc., 2nd ed., 2000.

[4] R. N. Bracewell, *The Fourier Transform and Its Applications*, New York: McGraw-Hill, 2nd ed., 1978

[5] A. V. Oppenheim, R. W. Schafer, and J. Buck, *Discrete-Time Signal Processing*, New Jersey: Prentice Hall, 1998.

[6] L. R. Soares and H. M. de Oliveira, "Fault Analysis Using Gegenbauer Multiresolution Analysis," in *Proc. of the 2004 IEEE Transmission and Distribution Latin America Conference (T&D2004 Latin America)*, São Paulo, Brazil, Nov. 2004.

[7] A. R. van C. Warrington, *Protective Relays: their Theory and Practice*, New York: John Wiley & Sons, Inc, vol. 1, 2. ed., 1968.

[8] B. Kasztenny, B. Campbell, and J. Mazereeuw, "Phase Selection for Single-Pole Tripping – Weak Infeed Conditions and Cross-Country Faults," in *Proc. of the 27th Annual Western Protective Relay Conference*, Spokane, Oct. 24-26, 2000.

[9] J. L. J. Driesen and R. J. M. Belmans, "Wavelet-Based Power Quantification Approaches," *IEEE Transactions on Instrumentation and Measurement*, vol. 52, no. 4, pp. 1232-1238, Aug. 2003.

VI. Biographies

Luciana R. Soares (S'2004) was born in Rio de Janeiro, Brazil, on May 30, 1973. She received the B.Sc and M.Sc degrees in electrical engineering from Universidade Federal de Pernambuco (UFPE), Recife, Brazil, in 1997 and 2001. Currently, she is a D.Sc. candidate at the Department of Electronics and Systems at same university (DES-UFPE).

Her special fields of interest include power quality monitoring and analysis, electromagnetic compatibility, fault analysis, wavelets, and applications of wavelet transforms on power system.

Hélio M. de Oliveira (M'1994) was born in Arcoverde, Pernambuco, Brazil, on May 1, 1959. He received the B.Sc. and M.S.E.E. degrees in electrical engineering from Universidade Federal de Pernambuco (UFPE), Recife, Brazil, in 1980 and 1983. Since 1983 he has been with the Department of Electronics and Systems (DES-UFPE). In 1992 he earned the *Docteur* degree from *École Nationale Supérieure des Télécommunications*, Paris.

Dr. de Oliveira was appointed as honored professor by about 20 undergraduate classes and authored the book *Análise de Sinais para Engenheiros: Wavelets* (Signal Analysis for Engineering: Wavelets). His research topics include communication theory, information theory and signal analysis. He is member of IEEE and SBrT (Brazilian Telecommunication Society).

Renato J. de Sobral Cintra was born in Recife, Pernambuco, Brazil. He received the B.Sc., M.Sc. and D.Sc. degrees all in electrical engineering from Universidade Federal de Pernambuco (UFPE), Recife, Brazil. During 2003-2004, he was research assistant at the University of Calgary, Canada. Since 2005 he has been with the Department of Statistics at UFPE. His fields of interest include non-conventional transform techniques, digital signal processing, and biological signal processing.